Ab Initio MO Study of Silver Ion Complexation in [2.2.2]Cyclophane π-Prismands

Pauli Saarenketo,[†,‡] Reijo Suontamo,[†] Tim Jödicke,[†,‡] and Kari Rissanen*[,†]

Department of Chemistry, University of Jyväskylä, P.O. Box 35, Survontie 9, FIN-40351, Jyväskylä, Finland, and Organisch-Chemisches Institut, Westfälische Wilhelms Universität Münster, Corrensstrasse 40, D-48149 Münster, Germany

Received February 28, 2000

Ab initio Hartree−Fock and DFT MO calculations have been used to study the conformations of [2.2.2]cyclophane π-prismands and the formation of π-complexes with silver ion and [2.2.2]cyclophanes. The lowest energy cyclophane conformations have been calculated up to the HF/6-31+G* level of theory. The silver π-complexes of the lowest energy conformations have been calculated with HF/3-21G* and B3LYP/3-21G* levels of theory. The nature of bonding in silver ion π-complexes has been studied with natural bond orbital analysis (NBO). Energies of the calculated cyclophanes and complexes, together with formation energies of those complexes, have also been discussed. The results obtained have been compared to X-ray crystal structures whenever such structures were available. Calculated and experimental X-ray structures agreed reasonably well given provision to the rather small 3-21G* basis set and the omission of triflate anion in the calculation model. The NBO analysis showed that when Ag^+ is bonded to the cyclophane cavity, the bonds are formed by σ-donation and d−π*-back-donation between the silver ion and the hydrocarbon skeleton, resulting in hexahapto ($3\times\eta^2$) overall π-bonding. This is in agreement with the well-known "bonding−back-bonding" scheme in transition metal carbonyl complexes. In this case the σ-donation from hydrocarbon to silver ion is the main contribution to the metal−cyclophane bonding. One dihapto (η^2) bonding to one aromatic ring in the present π-prismands relates by strength to a single strong hydrogen bond, which is up to 100 kJ/mol; thus the strength of this $3\times\eta^2$ bonding in these [2.2.2]cyclophane π-prismands can be compared to three simultaneous strong hydrogen bonds.

Introduction

Polycyclic aromatic hydrocarbons form complexes with metal ions such as Ag^+. Bonding in these π-complexes is due to electron transfer between the aromatic moiety and the positively charged metal cation.[1] Vögtle et al.[2] showed that concave hydrocarbons can extract certain metal cations from an aqueous solution. The complexation selectivity of the hydrocarbon cyclophanes allows applications such as incorporation in ion-selective electrodes. A number of cyclophanes were tested as ionophores, and as a result, the PVC-[2.2.2]paracyclophane membrane showed a remarkable selectivity toward silver and against alkali-metal, alkaline-earth-metal, and thallium ions.[2] The well-known [2.2.2]*p*,*p*,*p*-cyclophane (**1**) is a member of the [2.2.2]cyclophane π-prismands. The structurally isomeric [2.2.2]*m*,*p*,*p*-(**2**) and [2.2.2]*m*,*m*,*p*-cyclophane (**3**) have also shown similar complexing ability with the silver ion.[3,4] The [2.2.2]-*m*,*m*,*m*-cyclophane (**4**) has not yet been tested for complexation.

Pierre et al.[5] prepared the [2.2.2]*p*,*p*,*p*-cyclophane (**1**) by the modified Wurtz condensation of paraxylylene chloride in the presence of a catalytic amount of tetraphenylethylene.[6] The open-chain compound was also obtained in the reaction. Complexation studies[5] showed that silver trifluoromethanesulfonate (Ag-triflate) and **1** form an extraordinarily stable 1:1 complex, where the Ag^+ cation is located inside the cyclophane cavity consisting of the three aromatic rings. Owing to its spatial shape and the complexing ability of **1**, the name "π-prismand"[5] was proposed for such hydrocarbon cyclophanes. Later X-ray crystallographic studies by Boekelheide et al.[7] verified that the silver ion in the **1**−Ag-triflate complex is located on the 3-fold axis, outside of the π-prismand cavity, of the original hydrocarbon. This structure facilitates a dihapto (η^2) Ag−C interaction with one carbon−carbon double bond on

* Corresponding author. E-mail: Kari.Rissanen@jyu.fi.
† University of Jyväskylä.
‡ Westfälische Wilhelms Universität Münster.

(1) (a) Atwood, J. L.; Davies, J. E. D.; MacNicol, D. D.; Vögtle, F. *Comprehensive Supramolecular Chemistry*; Pergamon: Oxford, 1996; Vol. 1. (b) Vögtle, F.; Seel, C.; Windscheif, P.-M. *Comprehensive Supramolecular Chemistry*; Pergamon: Oxford, 1996; Vol. 2, p 211.
(2) Gross, J.; Harder, G.; Siepen, A.; Harren, J.; Vögtle, F.; Stephan, H.; Gloe, K.; Ahlers, B.; Cammann, K.; Rissanen, K. *Chem. Eur. J.* **1996**, *2*, 1585.
(3) Seppälä, T.; Wegelius, E.; Rissanen, K. *New. J. Chem.* **1998**, *22*, 789.
(4) Lahtinen, T.; Wegelius, E.; Airola, K.; Kolehmainen, E.; Rissanen, K. *J. Prakt. Chem.* **1999**, *341*, 237.
(5) Pierre, J.-L.; Baret, P.; Chautemps, P.; Armand, M. *J. Am. Chem. Soc.* **1981**, *103*, 2986.
(6) Tabushi, I.; Yamada, H.; Yoshida, Z.; Oda, R. *Tetrahedron* **1971**, *27*, 4845.
(7) Kang, H. C.; Hanson, A. W.; Eaton, B.; Boekelheide, V. *J. Am. Chem. Soc.* **1985**, *107*, 1979.

10.1021/om000190m CCC: $19.00
Publication on Web 05/17/2000

each phenyl moiety, leading to hexahapto ($3\times\eta^2$) overall π-bonding between the silver ion and **1**.

The mechanism of the π-bonding between the aromatic ring and silver ion in the case of bis(*m*-xylene)-silver perchlorate has been discussed by Taylor et al.[8] In the case of electron donation from the aromatic to the metal acceptor orbitals, the best position for the metal ion would be in the π-cloud above one of the carbon atoms of the ring, the position of the highest π-electron density. While in the case of electron back-donation from metal to aromatic moiety the best overlap between the filled metal d-orbitals and the antibonding π MOs of the aromatic moiety is achieved with the metal in the π-cloud equidistant between two carbon atoms of the ring.

Boekelheide et al.[7] found that the gas-phase dimerization of benzocyclobutenes in a nitrogen stream was an efficient method for making dibenzocyclooctadienes. When benzo[1,2;4,5]dicyclobutene was used under similar conditions, [2_4](1,2,4,5)cyclophane was obtained. Increasing the concentration of benzo[1,2;4,5]dicyclobutene in the hot zone of the pyrolysis tube produced finally [2_6](1,2,4,5)cyclophane (deltaphane) (**5**), which would be an ideal π-prismand.[7]

We have recently reported the synthesis of **2** and **3** based on cyclophane methodology where sulfide cyclization is done under high dilution followed by oxidation and sulfone pyrolysis.[9,10] The X-ray structures of **2**−Ag- and **3**−Ag-triflate show similar π-bonding between the silver ion and cyclophane ligand as in **1**−Ag-triflate complex, despite ring size reduction and conformational isomerism.[3,4]

Preparation of [2.2.2]*m*,*m*,*m*-cyclophane (**4**) as a side product of the Wurtz reaction has been reported by Jenny and Burri[11] in 1966. The structure of **4** was only briefly proved by mass spectrometry and NMR.

In this paper, we report ab initio Hartree−Fock and DFT MO calculations of cyclophanes **1**, **2**, **3**, and **4** and their π-complexes with a silver ion in order to gain further information about the bonding nature of these π-prismands. Nonbonded contact distances between carbon atoms closest to the silver ion, angles, and torsion angles of optimized conformations are compared to the X-ray diffraction structures when available. The nature of bonding is studied with natural bond orbital analysis (NBO).[12] Energies of calculated ligands and complexes, as well as formation energies of these complexes, are also discussed.

Experimental Section

The most stable conformations of very flexible free cyclophanes **1**−**4** were searched for using a systematic search method with molecular mechanics using the Cerius[2] computer program[13] and pcff force field.[14] Molecular dynamics simulation was performed for all conformations found, at temperatures of 400 and 600 K under the constant-energy and constant-volume ensemble (NVE).[15] The length of each simulation was 20 000 steps in 0.001 ps time steps. Dynamics simulation provided the molecule with enough energy to cross potential-energy barriers between conformations. During the dynamics simulation, conformations were minimized after every 1000 steps using a quenched dynamics method to collect all possible conformations. Four conformations were found for cyclophane **1**, 10 for cyclophane **2**, 19 for cyclophane **3**, and 12 for cyclophane **4**.

Each conformation of the cyclophanes **1**−**4** that was found was optimized by using the HF/STO-3G level of theory. Between two and four of the most stable HF/STO-3G conformations of each cyclophane **1**−**4** were calculated at the HF/3-21G* level of theory. These structures were further optimized at the B3LYP/3-21G*[16] and HF/6-31+G* levels of theory. A silver cation (Ag^+) was placed in the cavity of HF/6-31+G* optimized ligands, and Hartree−Fock and DFT methods were used along with the 3-21G* basis set to optimize these complexes. The larger 6-31+G* basis set was not available for the silver atom. For the most stable silver complexes a single-point NBO (natural bond orbital)[12] calculation was performed. Møller−Plesset electron correlation (MP2) was not used for optimization because of the sizes of the complexes and limited calculation resources. All semiempirical and ab initio MO calculations were performed with the Gaussian 94 series of programs.[17] As the application of effective core potentials is discussed in the literature, we used one method described,[18] but due to convergence problems we came back to the all-electron methods.

Results and Discussion

The Cyclophanes. The structurally isomeric cyclophanes **1**−**4** (see Figure 1) each have the same $C_{24}H_{24}$ skeleton, but ring size is changed from the 18-membered ring of **1** to the 15-membered ring of **4**. The reduction of the ring size is caused by the change of the spatial connections inside the isomeric skeleton.

Energies of the most stable conformations of the calculated cyclophanes are shown in Table 1. The energy difference between the most stable conformations of separate isomeric cyclophanes is shown in Table 2 and is rather small. HF/6-31+G* energy differences are somewhat smaller than those with 3-21G* basis sets, but the relative order is qualitatively identical with all levels of theories. The cyclophane **1** is highest, and the ligand **4** is lowest in energy.

Energy differences between conformations of a single cyclophane isomer are small, as shown in Table 2. The calculated HF/3-21G* bond parameters of free cyclophanes are presented in Table 3. They show that the

(8) Taylor, I. F., Jr.; Hall, E. A.; Amma, E. L. *J. Am. Chem. Soc.* **1969**, *91*, 5745.
(9) Laufenberg, S.; Feuerbacher, N.; Pischel, I.; Börsch, O.; Nieger, M.; Vögtle, F. *Liebigs Ann. Chem.* **1997**, 1901.
(10) Vögtle, F. *Cyclophane Chemistry*; Wiley: Chichester, 1993.
(11) Jenny, W.; Burri, K. *Chimia* **1966**, *20*, 436.
(12) (a) Reed, A. E.; Weinstock, R. B.; Weinhold, F. *J. Chem. Phys.* **1985**, *83*(2), 735. (b) Reed, A. E.; Curtiss, L. A.; Weinhold, F. *Chem. Rev.* **1988**, *88*, 899. (c) Glendening, E. D.; Reed, A. E.; Carpenter, J. E.; Weinhold, F. *NBO Version 3.1*.
(13) *Cerius[2] Conformational Search and Analysis*; Molecular Simulations Inc.: San Diego, 1997; p 2.
(14) *Forcefield-Based Simulations General Theory & Methodology*; Molecular Simulations Inc.: San Diego, 1997; p 29.
(15) *Forcefield-Based Simulations General Theory & Methodology*; Molecular Simulations Inc.: San Diego, 1997; p 208.
(16) (a) Becke, A. D. *J. Chem. Phys.* **1993**, *98*, 5648. (b) Becke, A. D. *Phys. Rev. B* **1988**, *37*, 3098. (c) Lee, C.; Yang, W.; Parr, R. G. *Phys. Rev. B* **1988**, *37*, 785.
(17) Frisch, M. J.; Trucks, G. W.; Schlegel, H. B.; Gill, P. M. W.; Johnson, B. G.; Robb, M. A.; Cheeseman, J. R.; Keith, T.; Petersson, G. A.; Montgomery, J. A.; Raghavachari, K.; Al-Laham, M. A.; Zakrzewski, V. G.; Ortiz, J. V.; Foresman, J. B.; Cioslowski, J.; Stefanov, B. B.; Nanayakkara, A.; Challacombe, M.; Peng, C. Y.; Ayala, P. Y.; Chen, W.; Wong, M. W.; Andres, J. L.; Replogle, E. S.; Gomperts, R.; Martin, R. L.; Fox, D. J.; Binkley, J. S.; Defrees, D. J.; Baker, J.; Stewart, J. P.; Head-Gordon, M.; Gonzalez, C.; Pople, J. A. *Gaussian 94*; Gaussian, Inc.: Pittsburgh, PA, 1995.
(18) Huang, H. Y.; Padin, J.; Yang, R. T. *J. Phys. Chem. B* **1999**, *103*, 3206.

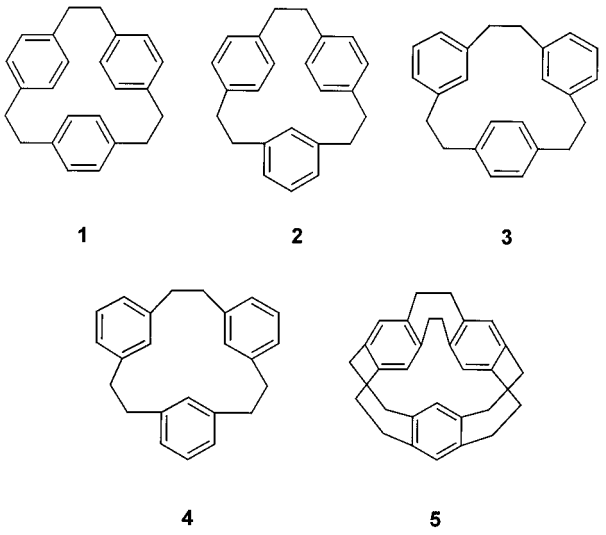

Figure 1. Cyclophanes **1**−**5**.

Table 1. Energies of the Most Stable Conformations of [2.2.2]Cyclophanes Calculated with Different Levels of Theory

structure	sym[a]	HF/3-21G* energy, au	HF/6-31+G* energy, au	B3LYP/3-21G* energy, au
1a	C_1	−917.700344	−922.854801	−923.942889
1b	C_2	−917.699108	−922.853361	−923.942213
2a	C_1	−917.707539	−922.860746	−923.949246
2b	C_1	−917.705701	−922.855717	−923.948433
2c	C_1	−917.701295	−922.854588	−923.944065
3a	C_2	−917.711303	−922.864658	−923.951895
3b	C_1	−917.710328	−922.863723	−923.951713
3c	C_1	−917.707665	−922.860007	−923.949062
3d	C_1	−917.705371	−922.858431	−923.947501
4a	C_1	−917.712238	−922.865315	−923.953085
4b	C_2	−917.712780	−922.863739	−923.954117
4c	C_3	−917.703234	−922.859421	−923.945321
4d	C_1	−917.707613	−922.859362	−923.949548

[a] Symmetries are taken from the HF/6-31+G* calculations.

Table 2. Energy Differences of the Lowest Energy Cyclophanes and Conformations

	HF/3-21G*		HF/6-31+G*		B3LYP/3-21G*	
structure	ΔE,[a] kJ/mol	ΔE,[b] kJ/mol	ΔE,[a] kJ/mol	ΔE,[b] kJ/mol	ΔE,[a] kJ/mol	ΔE,[b] kJ/mol
1a	0	32.7	0	27.6	0	29.5
1b	3.25		3.79		1.78	
2a	0	13.8	0	12.0	0	12.8
2b	4.83		13.2		2.13	
2c	16.4		16.2		13.6	
3a	0	3.88	0	1.73	0	5.83
3b	2.56		2.46		0.48	
3c	9.56		12.2		7.44	
3d	15.6		16.4		11.3	
4a	1.42		0	0	2.71	
4b	0	0	4.14		0	0
4c	25.1		15.5		23.1	
4d	13.6		15.6		12.0	

[a] ΔE energies are relative to the energy of the lowest energy conformation. [b] ΔE energies are relative to the energy of the lowest energy cyclophane.

structural differences resulting in conformations of different point group symmetries (Table 1) are mainly due to changes in torsion angles of bridging ethane building blocks. Small energy differences in conformations of individual cyclophane isomers and substantial fluctuations in torsion angles indicate that cyclophanes **1**−**4** are quite flexible and thus capable of adapting to

Table 3. Bond Parameters (in pm and deg) of Cyclophanes 1−4 Calculated with the HF/3-21G* Level of Theory

1	**1a**	**1b**	**2**	**2a**	**2b**	**2c**	**3**	**3a**	**3b**	**3c**	**3d**	**4**	**4a**	**4b**	**4c**	**4d**
22−1	151.9	152.0	23−1	151.9	152.2	151.9	22−1	151.5	151.4	151.4	151.2	23−1	151.7	151.7	152.1	151.8
1−2	155.6	155.8	1−2	155.1	156.2	155.3	1−2	152.2	155.4	155.5	155.6	1−2	155.2	155.5	154.9	155.5
2−3	151.9	151.8	2−3	152.0	151.7	151.8	2−3	151.8	151.7	151.8	151.9	2−3	151.7	151.7	151.9	152.0
6−9	151.9	151.8	6−9	151.7	151.5	151.8	7−9	151.9	152.1	152.8	151.9	7−9	152.2	152.0	152.1	152.1
9−10	155.6	155.5	9−10	156.0	156.3	156.4	9−10	155.5	154.6	154.3	155.8	9−10	155.3	155.5	154.9	157.2
10−11	151.9	151.8	10−11	151.6	151.5	151.5	10−11	151.9	152.2	152.8	152.2	10−11	151.7	151.8	151.9	152.0
14−17	151.9	151.8	14−17	151.4	151.7	152.3	15−17	151.8	151.8	151.8	152.5	15−17	151.8	151.8	152.1	151.7
17−18	155.6	155.8	17−18	155.4	156.2	154.2	17−18	155.2	155.5	155.5	154.9	17−18	155.1	155.5	154.9	155.7
18−19	151.9	152.0	18−19	152.0	152.2	152.8	18−19	151.5	151.4	151.4	151.8	18−19	151.7	152.0	151.9	151.7
22−1−2	113.7	114.2	23−1−2	114.2	114.8	113.9	22−1−2	112.0	111.7	111.3	110.8	23−1−2	112.8	112.7	115.0	112.7
1−2−3	113.7	113.5	1−2−3	114.4	112.0	113.5	1−2−3	113.0	112.7	112.5	112.7	1−2−3	113.2	112.7	114.1	114.1
6−9−10	113.7	113.7	6−9−10	112.4	111.4	112.7	7−9−10	113.9	115.4	117.3	114.3	7−9−10	114.6	113.7	115.0	113.6
9−10−11	113.7	113.7	9−10−11	112.2	111.4	111.7	9−10−11	113.9	116.6	117.3	114.5	9−10−11	113.6	113.4	114.1	112.5
14−17−18	113.7	113.5	14−17−18	112.3	112.0	115.9	15−17−18	113.0	112.7	112.5	116.2	15−17−18	113.3	113.4	115.0	112.2
17−18−19	113.7	114.2	17−18−19	114.0	114.8	117.0	17−18−19	112.0	112.0	111.3	113.7	17−18−19	113.3	113.7	114.1	112.7
23−22−1−2	−53.6	−45.6	22−23−1−2	−76.7	112.8	−70.2	23−22−1−2	−67.5	−99.4	−103.7	−93.4	22−23−1−2	−66.6	−70.7	−134.1	−111.8
5−6−9−10	−53.6	−118.0	5−6−9−10	−61.3	−70.5	−64.4	6−7−9−10	73.7	−55.0	171.6	−95.2	6−7−9−10	58.7	117.9	−134.1	114.4
15−14−17−18	−53.6	−69.5	15−14−17−18	−93.0	−102.0	−10.8	14−15−17−18	−68.7	−67.0	75.3	152.0	14−15−17−18	−61.0	−106.4	−134.1	−69.6
22−1−2−3	−48.4	−48.1	23−1−2−3	−63.4	85.6	−69.1	22−1−2−3	−58.4	60.9	60.4	61.5	23−1−2−3	−67.7	−60.6	55.7	67.1
6−9−10−11	−48.4	48.1	6−9−10−11	−46.6	−47.8	−41.2	7−9−10−11	82.3	−67.4	34.5	−86.0	7−9−10−11	76.1	−66.2	55.7	105.3
14−17−18−19	−48.4	−48.1	14−17−18−19	64.7	85.6	−59.2	15−17−18−19	−58.4	−62.2	60.4	−49.2	15−17−18−19	−58.1	−66.2	55.7	−56.1

Table 4. Energies of π-Prismand−Ag Complexes

	HF/3-21G*				B3LYP/3-21G*			
complex	energy, au	ΔE,[a] kJ/mol	ΔE,[b] kJ/mol	ΔH(cf),[c] kJ/mol	energy, au	ΔE,[a] kJ/mol	ΔE,[b] kJ/mol	ΔH(cf),[c] kJ/mol
1a−Ag^+	−6091.425621	0	16.6	−327.4	−6100.133207	0	19.6	−424.2
1b−Ag^+	−6091.423344	6.0		−324.7	−6100.128831	11.5		−414.4
2a−Ag^+	−6091.430298	0	4.31	−320.8	−6100.138269	0	6.60	−420.8
2c−Ag^+	−6091.422370	20.8		−316.3	−6100.133365	12.9		−421.5
2b−Ag^+	−6091.422313	21.0		−304.8	−6100.134486	9.9		−413.0
3b−Ag^+	−6091.431939	0	0	−317.8	−6100.140789	0	0	−420.9
3a−Ag^+	−6091.427501	11.7		−303.6	−6100.139303	3.9		−416.5
3d−Ag^+	−6091.415861	42.2		−288.6	−6100.131554	24.2		−407.7
3c−Ag^+	−6091.410708	55.8		−269.1	−6100.127930	33.8		−394.1
4c−Ag^+	−6091.427876	0	10.7	−325.8	−6100.132994	9.3		−417.2
4d−Ag^+	−6091.427826	0.1		−314.2	−6100.133627	7.7		−407.8
4a−Ag^+	−6091.424358	9.2		−292.9	−6100.136543	0	11.1	−406.1
4b−Ag^+	−6091.411994	41.7		−259.0	−6100.123816	33.4		−370.0
Ag^+	−5173.600559				−5176.028766			

[a] ΔE energies are relative to energy of the lowest energy conformation. [b] ΔE energies are relative to energy of the lowest energy complex. [c] $\Delta H(\text{cf}) = E([(\pi\text{-prismand})\text{Ag}]^+) - E(\text{Ag}^+) - E(\pi\text{-prismand})$.

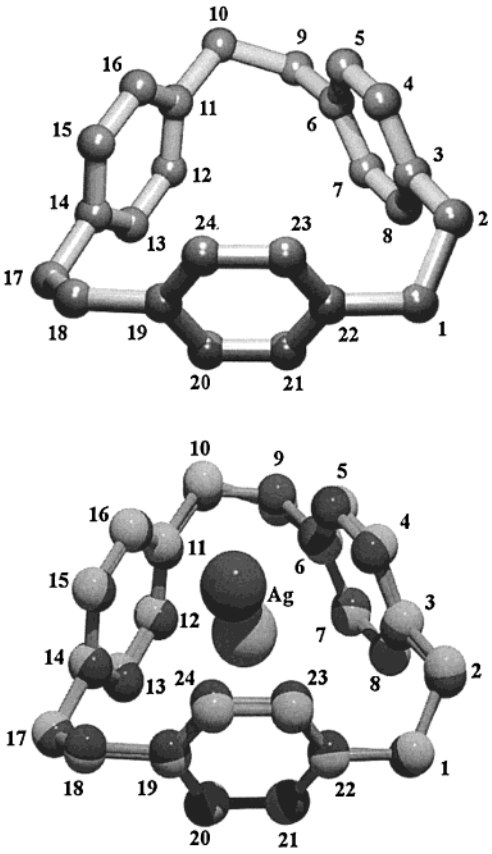

Figure 2. Structures of **1a** and **1a**−Ag^+ complex (light gray) and an X-ray structure of **1**−Ag-triflate (dark gray) complex. Structures of **1a** and **1a**−Ag^+ complex were calculated with the HF/3-21G* level of theory. Hydrogen atoms and the triflate anion are omitted for clarity.

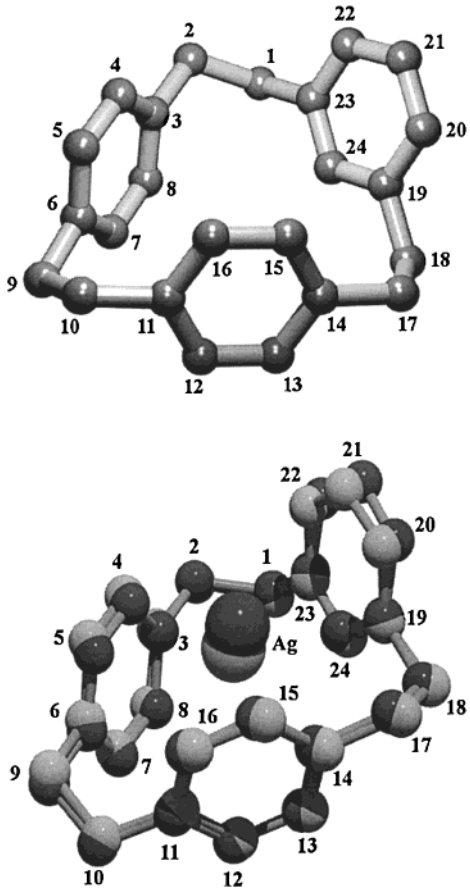

Figure 3. Structures of **2a** and **2a**−Ag^+ complex (light gray) and an X-ray structure of **2**−Ag-triflate (dark gray) complex. Structures of **2a** and **2a**−Ag^+ complex were calculated with the HF/3-21G* level of theory. Hydrogen atoms and the triflate anion are omitted for clarity.

various environments when complexing with metal ions. The most stable conformations of different cyclophanes calculated with the HF/3-21G* level of theory are depicted in Figures 2−5.

The Ag Complexes. Table 4 shows energies of the π-prismand−Ag complexes calculated with the HF/3-21G* and B3LYP/3-21G* levels of theory. The order of increasing energy changes due to complex formation. For all ligands, the complexation causes slightly larger energy differences between the ligand conformations when compared to the energy differences of the corresponding free cyclophane conformations. The complexation with silver retains the lowest energy conformations of **1a** and **2a**, while the lowest energy conformation of **3** changes from **3a** to **3b**. When calculated with the HF method, the lowest energy conformation of **4** changes from **4b** to **4c**, while application of the DFT method changes from **4b** to **4a**. This difference between the methods is only true for the absolute values of the energy difference (ΔE), while the complex formation energies (ΔH(cf)) are showing similar order of energy

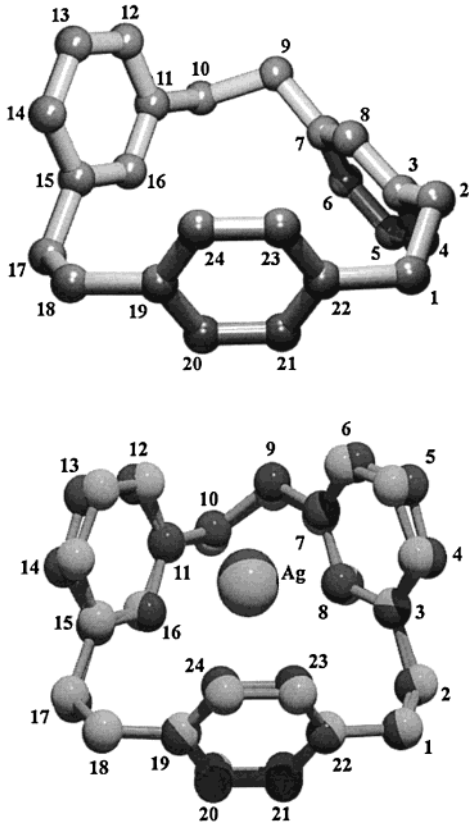

Figure 4. Structures of **3a** and **3b**−Ag^+ complex (light gray) and an X-ray structure of **3**−Ag-triflate (dark gray) complex. Structures of **3a** and **3b**−Ag^+ complex were calculated with the HF/3-21G* level of theory. Hydrogen atoms and the triflate anion are omitted for clarity.

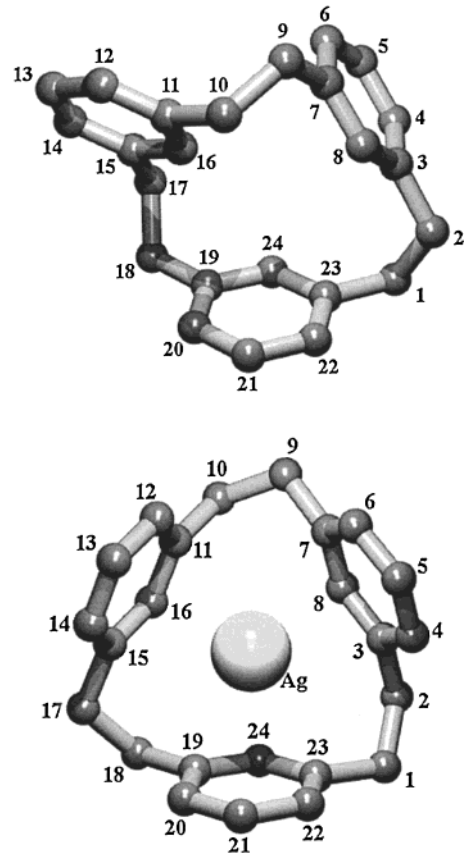

Figure 5. Structures of **4b** and **4c**−Ag^+ complex calculated with the HF/3-21G* level of theory. Hydrogen atoms are omitted for clarity.

with the **4c**−Ag^+ complex as the lowest energy conformation. The formation of this complex favors higher free ligand C_3 symmetry. On the other hand, for cyclophane **3**, formation of **3b**−Ag^+ indicates the opposite trend, favoring the **3b** C_1 free ligand symmetry instead of higher **3a** C_2 symmetry. The energy differences between the lowest energy conformations of **1**−**4**−Ag complexes are also shown in Table 4. The energy order is different compared with the free ligand energy order, and the energy differences are even less than for the free ligands. The absolute values of these energy differences are very small, but still one can discuss the trends.

The effect of bonding due to complexation can be estimated by calculating the complex formation energy ΔH(cf) for the hypothetical reaction $Ag^+ + \pi$-prismand → [(π-prismand)Ag]$^+$ with the formula $\Delta H(\text{cf}) = E([(\pi\text{-prismand})\text{Ag}]^+) - E(\text{Ag}^+) - E(\pi\text{-prismand})$. The energy values of the corresponding conformations are used in the formula. Calculated ΔH(cf) values are given in Table 4, and they all are negative, e.g., exothermic, favoring the formation of silver complexes. The order of decreasing stability is **1a**−Ag^+ → **2a**−Ag^+ → **3b**−Ag^+ → **4c**−Ag^+.

The overall increase in stability as a result of the complex formation is reflected as lowering of the energy of the bonding MOs as shown for **2a** and **2a**−Ag^+ in Figure 6 as an example. A contour plot of the HOMO orbital in both free cyclophane and the complex is included in the MO energy diagrams. It can be seen that the bonding of Ag^+ ion to the ligand does not radically

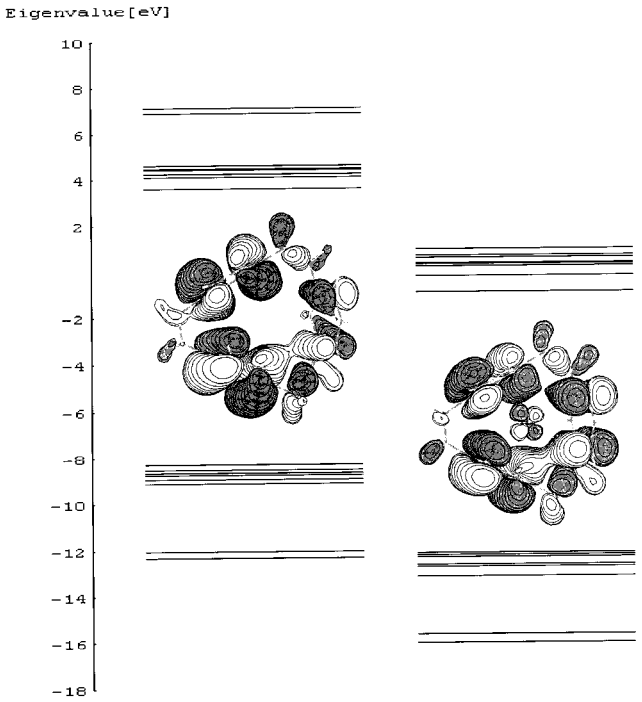

Figure 6. Eigenvalues of cyclophane **2a** (left) and complex **2a**−Ag^+ (right) calculated with the HF/3-21G* level of theory. The HOMO orbitals at contour level 0.04 are shown in the middle pictures.

alter the shape of the HOMO orbital. The 4d-orbital of the silver ion is shown in the plot.

The structures of the lowest energy conformations of

Table 5. Bond Distances (pm) and Angles (deg) of 1a and 1a−Ag$^+$ Complex and an X-ray Structure of 1−Ag-triflate Complex

	HF/3-21G*		B3LYP/3-21G*		X-ray diffraction
	1a	**1a**−Ag$^+$	**1a**	**1a**−Ag$^+$	**1**−Ag-triflate
Ag−C(4)		283.0		255.4	255.4
Ag−C(5)		286.0		261.0	269.7
Ag−C(15)		286.0		261.0	262.8
Ag−C(16)		283.0		255.3	261.9
Ag−C(23)		286.0		260.7	262.8
Ag−C(24)		283.0		255.3	256.3
C(7)−C(5)−Ag		70.6		88.0	96.7
C(13)−C(15)−Ag		70.6		88.0	96.2
C(21)−C(23)−Ag		70.6		88.1	92.0
C(3)−C(6)−Ag		60.4		60.8	59.8
C(11)−C(14)−Ag		60.4		60.8	64.0
C(19)−C(22)−Ag		60.4		60.8	62.0
C(23)−C(22)−C(1)−C(2)	−53.6	−55.7	−52.8	−49.9	−54.8
C(5)−C(6)−C(9)−C(10)	−53.6	−55.7	−52.3	−50.0	−49.0
C(15)−C(14)−C(17)−C(18)	−53.6	−55.7	−53.3	−49.9	−73.4
C(22)−C(1)−C(2)−C(3)	−48.4	−48.9	−49.5	−47.6	−52.4
C(6)−C(9)−C(10)−C(11)	−48.4	−48.9	−49.0	−47.6	−49.3
C(14)−C(17)−C(18)−C(19)	−48.4	−48.9	−49.4	−47.6	−23.3

Table 6. Bond Distances (pm) and Angles (deg) of 2a and 2a−Ag$^+$ Complex and an X-ray Structure of 2−Ag-triflate Complex

	HF/3-21G*		B3LYP/3-21G*		X-ray diffraction
	2a	**2a**−Ag$^+$	**2a**	**2a**−Ag$^+$	**2**−Ag-triflate
Ag−C(4)		269.2		252.1	257.3
Ag−C(5)		286.8		261.2	277.7
Ag−C(14)		297.9		279.6	279.9
Ag−C(15)		267.5		254.3	254.2
Ag−C(19)		290.2		280.5	278.4
Ag−C(24)		265.8		249.6	258.7
C(7)−C(5)−Ag		77.8		88.2	95.3
C(13)−C(15)−Ag		82.3		80.4	87.4
C(24)−C(21)−Ag		49.2		43.8	46.7
C(3)−C(6)−Ag		56.5		59.6	58.0
C(11)−C(14)−Ag		64.4		67.7	78.2
C(19)−C(23)−Ag		65.7		63.0	60.6
C(22)−C(23)−C(1)−C(2)	−64.7	−60.6	−63.0	−64.5	−75.4
C(5)−C(6)−C(9)−C(10)	−110.3	−123.4	−102.6	−113.5	−113.9
C(15)−C(14)−C(17)−C(18)	−125.2	−123.8	−124.2	−116.1	−123.9
C(23)−C(1)−C(2)−C(3)	−63.0	−59.4	−65.4	−60.1	−62.2
C(6)−C(9)−C(10)−C(11)	45.5	44.9	48.1	45.4	37.3
C(14)−C(17)−C(18)−C(19)	62.9	60.0	63.5	60.8	64.5

different silver ion complexes are presented in Figures 2−5. When X-ray structures were available, a superposition image is shown for sake of comparison. Tables 5−8 contain selected experimental (for instance, the six shortest Ag−C bond distances) and corresponding calculated bond parameters for the π-prismand−Ag complexes studied here. The pictures shown in Figure 2−5 are the results of the HF/3-21G* calculations.

As seen in Figure 2, complexation of the silver ion to the lowest energy conformation **1a** does not lead to a significant change in the conformation of the ligand in **1a**−Ag$^+$. This is also shown by similar torsion angle values in Table 5. In all of the calculated and experimental structures of the **1**−Ag complex, the silver ion is bonded with the three shortest bonds to the carbon atoms (C4, C16, and C24) in separate phenyl rings. This and C−C−Ag angles in Table 5 show that Ag$^+$ is located at almost equal distances to three phenyl rings. In the HF-calculated structure (**1a**−Ag$^+$) the Ag$^+$ ion is located in the center of the π-prismand, while in the experimental X-ray (**1**−Ag-triflate) and the DFT-calculated structure (Table 5) the silver ion is at the upper edge of the π-prismand cavity. This is indicated by the shorter Ag−C bonding distances and larger C−C−Ag angles in the X-ray structure. The ethane bridge formed by the carbon atoms 17 and 18 in the calculated **1a**−Ag$^+$ complexes is slightly differently oriented when compared to the experimental **1**−Ag-triflate structure, as seen in the torsion angles of Table 5.

The complexation of the Ag$^+$ ion to **2a** slightly changes the conformation of the cyclophane in the **2a**−Ag$^+$ complex, as seen in Figure 3 and in the torsion angles in Table 6. In both the calculated (**2a**−Ag$^+$) and X-ray structure (**2**−Ag-triflate), the silver ion is bonded with the shortest Ag−C distances to one carbon atom (C4, C15, and C24) in each of the three phenyl rings of the ligand. In the HF-calculated complex, the silver ion is located slightly farther away from the carbon atoms than in the DFT-calculated and X-ray structure. The ethane bridges are orientated nearly the same in the calculated and in experimental structures. This can be deduced from Table 6 and Figure 3.

Figure 4 and Table 7 show that the lowest energy conformation **3a** is changed during formation of the

Table 7. Bond Distances (pm) and Angles (deg) of 3a and 3b−Ag$^+$ Complex and an X-ray Structure of 3−Ag-triflate Complex

	HF/3-21G*		B3LYP/3-21G*		X-ray diffraction
	3a	**3b**−Ag$^+$	**3a**	**3b**−Ag$^+$	**3**−Ag-triflate
Ag−C(7)		273.1		267.3	266.8
Ag−C(8)		274.6		249.1	255.8
Ag−C(11)		276.3		257.1	264.4
Ag−C(16)		275.8		251.3	260.7
Ag−C(23)		268.3		250.6	256.8
Ag−C(24)		270.0		253.2	257.5
C(8)−C(5)−Ag		52.0		43.5	44.9
C(16)−C(13)−Ag		53.0		44.1	46.0
C(21)−C(23)−Ag		88.0		88.3	97.9
C(3)−C(7)−Ag		73.6		70.1	73.2
C(11)−C(15)−Ag		59.1		54.0	54.4
C(19)−C(22)−Ag		63.7		62.7	64.0
C(23)−C(22)−C(1)−C(2)	−67.5	−109.4	−67.0	−97.9	−98.7
C(6)−C(7)−C(9)−C(10)	73.7	−127.9	73.2	−133.1	−146.5
C(14)−C(15)−C(17)−C(18)	−68.7	−75.3	−68.0	−74.9	−80.1
C(22)−C(1)−C(2)−C(3)	−58.4	57.3	−58.8	59.6	63.0
C(7)−C(9)−C(10)−C(11)	82.3	57.6	82.4	59.0	64.4
C(15)−C(17)−C(18)−C(19)	−58.4	−56.3	−58.8	−58.0	−61.4

Table 8. Bond Distances (pm) and Angles (deg) of 4b and 4c−Ag$^+$ Complex

	HF/3-21G*		B3LYP/3-21G*	
	4b	**4c**−Ag$^+$	**4b**	**4c**−Ag$^+$
Ag−C(3)		293.2		271.8
Ag−C(8)		281.9		246.1
Ag−C(11)		292.5		271.7
Ag−C(16)		281.8		246.9
Ag−C(19)		292.7		274.3
Ag−C(24)		282.5		245.5
C(8)−C(5)−Ag		55.1		42.7
C(16)−C(13)−Ag		55.0		43.3
C(24)−C(21)−Ag		55.4		42.5
C(3)−C(7)−Ag		65.1		60.8
C(11)−C(15)−Ag		64.9		60.9
C(19)−C(23)−Ag		64.9		61.8
C(22)−C(23)−C(1)−C(2)	−70.7	−128.4	−85.0	−130.9
C(6)−C(7)−C(9)−C(10)	117.9	−128.9	118.6	−130.6
C(14)−C(15)−C(17)−C(18)	−106.4	−129.0	−106.2	−128.9
C(23)−C(1)−C(2)−C(3)	−60.6	52.1	−60.8	54.3
C(7)−C(9)−C(10)−C(11)	−66.2	52.4	−66.3	53.9
C(15)−C(17)−C(18)−C(19)	−66.2	52.1	−66.3	53.3

Table 9. Results of the NBO Analysis at the HF/3-21G* Level of Theory

complex	C→M σ-donation[a]	M→C d−π*-back-donation[b]	net change
1a−Ag$^+$	0.099	−0.031	0.068
2a−Ag$^+$	0.099	−0.043	0.056
3b−Ag$^+$	0.095	−0.041	0.054
4c−Ag$^+$	0.090	−0.026	0.074

[a] The increase of electron population on valence s-orbitals of the metal. [b] The decrease of electron population on valence d-orbitals of the metal.

lowest energy complex **3b**−Ag$^+$. In free cyclophane **3a** the *meta*-bonded rings point in opposite directions, while in the calculated (**3b**−Ag$^+$) and the experimental (**3**−Ag-triflate) complex both *meta*-bonded aromatic rings are oriented in the same direction. In the HF-optimized **3a**−Ag$^+$ complex the silver is bonded almost equidistantly to the two *meta*-bonded phenyl rings, but is closest to carbons C23 and C24 in the *para*-bonded ring. Also, in the experimental **3**−Ag-triflate, the bonds Ag−C23 and Ag−C24 are among the three shortest bonds, but bond Ag−C8 to the *meta*-bonded ring is the shortest, as in the B3LYP-calculated structure.

In the lowest energy conformation **4b**, one *meta* phenyl ring is flipped outside of the π-prismand cavity, as illustrated in Figure 5 and Table 8. During formation of complex **4c**−Ag$^+$, the differently oriented aromatic rings of the free ligand are organized in a more symmetric orientation around Ag$^+$, as also shown in Figure 5 and Table 8. The silver ion is bonded with the three shortest Ag−C distances to one carbon in each phenyl ring (C8, C16, and C24) and so is located in the center of the almost symmetrical ligand cavity. In the B3LYP-optimized structure the Ag−C bonds are shorter. The X-ray structure is not available for the **4**−Ag$^+$ complex.

To test the bonding scheme proposed by Taylor et al.,[8] a natural bond orbital analysis (NBO)[12] was carried out for the complexes. In Table 9 a summary of this analysis is given. According to NBO analysis, the σ-donation was the main contribution to the Ag−cyclophane bonding in all complexes, and as can be seen from Tables 5−8, the silver cation in the calculated and in the X-ray structure is usually clearly closer to one of the two carbon atoms of each aromatic ring in the cyclophane skeleton. This is in agreement with the proposed bonding scheme of Taylor.

Ag$^+$ is shown to form weak bonds by getting electron density from the hydrocarbon skeleton to the empty 5s-orbital and partially donating electron pairs from its valence 4d-orbitals to the antibonding π-MOs of the three aromatic rings of the π-prismands, resulting in hexahapto ($3\times\eta^2$) overall π-bonding between the silver ion and the π-prismand. This model of π-complexation was first proposed by Dewar[19] and applied by Chatt and Duncanson[20] in 1953.

The strength of the bond can be compared to a strong hydrogen bond. Hydrogen bonds are usually weak, typically 20−25 kJ/mol, but strong hydrogen bonds can go up to 100 kJ/mol[21] and are of the same order as one dihapto (η^2) bonding to one aromatic ring in the present π-prismands.

(19) Dewar, M. J. S. *Bull. Soc. Chim. Fr.* **1951**, *18C*, 71.
(20) Chatt, J.; Duncanson, L. A. *J. Chem. Soc.* **1953**, 2939.
(21) Shriver, D. F.; Atkins, P. W.; Langford, C. H. *Inorganic Chemistry*; Oxford University Press, 1994.

Conclusions

The present free cyclophanes are flexible, allowing twisting of the ethane linkages connecting the aromatic rings. This flexibility results in numerous, energetically nearly equivalent conformations. Calculated and experimental X-ray structures of the complexes agree reasonably well given provision to the 3-21G* basis set and the omission of the triflate anion in the calculation model. In these cases the B3LYP method reproduces the X-ray structures more accurately than the HF method. Complex formation was found to be exothermic, thus suggesting that the [2.2.2]*m*,*m*,*m*-cyclophane−AgY complex, despite being the least stable complex in the calculated series, might also be possible to prepare and that it should have a structure similar to the other π-prismand complexes studied here.

The NBO[12] analysis of the present π-complexes shows a rather normal bonding back-bonding behavior, although in most cases known in the literature[18,22] the bonding part comes mainly out of the d−π* back-bonding. In our complexes the σ-bonding aspect is dominant.

OM000190M

(22) Kovacs, A.; Frenking, G. *Organometallics* **1999**, *18*, 887.